Performance of Single Friction Pendulum bearing for isolated buildings subjected to seismic actions in Vietnam

N V Nguyen[1*], C H Nguyen[1], H P Hoang[2] and K T Huong[3]

[1]Department *of Civil Engineering, Industrial University of Ho Chi Minh City*, Vietnam
[2]The University of Danang, University of Science and Technology, Vietnam
[3]Ton Duc Thang University, Vietnam
[*]Corresponding author. Email: *nguyenvannam@iuh.edu.vn*

Abstract. Using structural control technology in earthquake resistant design of buildings in Vietnam is very limited. In this paper, a performance evaluation of using Single Friction Pendulum (SFP) bearing for seismically isolated buildings with earthquake conditions in Vietnam is presented. A two-dimensional (2-D) model of the 5-storey building subjected to earthquakes is analyzed in time domain. Accordingly, the model is analyzed for 2 cases: with and without SFP bearing. The ground acceleration data is selected and scaled to suit the design acceleration in Hanoi followed by the Standard TCVN 9386:2012. It is shown that the seismically isolated buildings gets the performance objectives while achieving an 91% reduction in the base shear, a significant decrease in the inter-story drift and absolute acceleration of each story.

1. Introduction

Earthquake is one of the major human dangers and the main cause of damage, collapse of constructions. Historically, there are many strong earthquakes occurring in many countries such as: Kanto (Japan, 1923), Sichuan (China, 2008)…, killing many people and causing heavy losses to their economies. Although Vietnam is not in the strong earthquake zone, strong earthquakes still occurred in history. Recently, earthquakes occur in Vietnam more frequently and stronger [1, 2]. The design of earthquake resistant buildings in Vietnam is limited with very simple theoretical models. The use of base isolation techonology in Vietnam is also rare. In this study, the use of a more modern isolation technology with SFP bearing for seismically isolated buildings in Vietnam is discussed.

Base isolation is a passive structural control technology, and is an effective approach to mitigate the damage caused by earthquakes to the structures. Recently, it has being studied and applied very commonly in developed countries such as USA, Japan…. The main idea of this technique is to isolate the superstructure from the ground by using flexible bearings, called seismic isolation bearings. It has a small horizontal stiffness and it is typically inserted between the foundation and superstructure to isolate the structure from the ground movement, detache the earthquake energy into the structure. With fixed-base structure, when earthquake happens, horizontal relative displacement between two stories is large. Hence, the risk of structural damage is high. Conversely, with base isolated structures, the superstructure is completely a rigid body and the inter-story drift of structure is significantly reduced. Base isolated structures will maintain the behavior in the elastic or near elastic region, and ensure that the structure is not damaged, as illustrated in Figure 1 [3].

Single Friction Pendulum (SFP) bearing is a popular device used in seismic base-isolation technology in recent years. It is first introduced in 1987 by Zayas [4]. It is made from stainless steel and it has a geometrical structure as shown in Figure 2. The bearing consists of an articulated slider sliding on a curved surface with a radius *R*. On the curved surface and slider are covered by a layer of Teflon material, which reduces the coefficient of friction between them (from 1% to 15%). The radius *R* in combination with the total weight of the superstructure *W* provides a horizontal stiffness of the bearing and restoring force to move the slider to the central position. At the same time, the friction coefficient of the bearing provides the initial horizontal stiffness to stabilize the bearing and dissipate a part of the earthquake energy when sliding occurs. The horizontal displacement capacity of the SFP bearing is *d*, as shown in Figure 2(b). The radius of the curved surface and coefficient of friction are important technical parameters of the bearing which decide the behavior of the bearing and the structure.

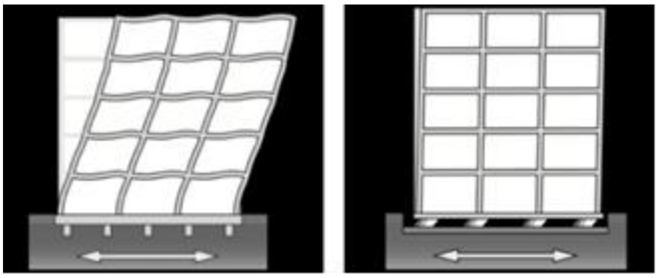

(a) (b)

Figure 1. Building subjected to earthquake excitation. (a) Non-isolated building, (b) Isolated building.

With this structure, the SFP bearing can be considered an improved type with many more advantages than previous types such as: rubber bearing, flat sliding bearing. The advantages include: durability and stability over time, resilience to the center at the end of earthquakes and easy adjustment to the technical parameters in the design.

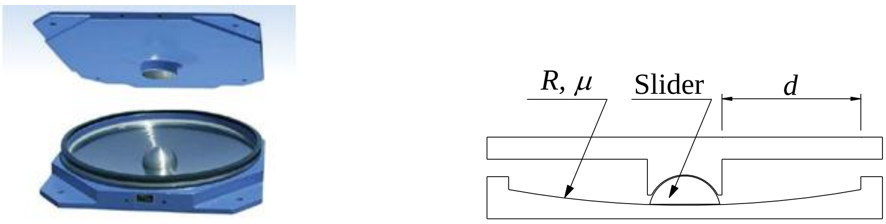

(a) (b)

Figure 2. Single friction pendulum (SFP) bearing. (a) Cutaway view, (b) Cross section.

2. Modeling of base-isolated buildings with SFP bearing

2.1. Force and horizontal displacement relationship of SFP bearing

The movement of bearing are described in detail in study of Zayas et al. (1987) [4]. When the ground motion is weak and the horizontal force in the bearing *F* is smaller than the friction force between the slider and the curved surface F_f, the sliding doesn't occurs. The base isolated structure, therefore, behaves like fixed base structure. Then the SFP bearing doesn't work, as shown Figure 2(b). When the ground motion is strong enough, the force *F* exceeds the friction force F_f, the sliding occurs, as shown Figure 3(a). During the motion, if the horizontal displacement *u* exceeds the displacement capacity of the bearing *d*, the circumferential hard boundary prevents the bearing displacement. The impact force F_r is provided to prevent sliding. The force components and horizontal displacements are shown in Figure 3(a). When the horizontal displacement of the slider is *u*, the relationship of force and horizontal displacement of the bearing is established on the basis of the force balance.

Considering equilibrium of the horizontal and vertical force at horizontal displacement *u* of the slider, the following relationships are obtained as follows, respectively:

$$F = F_n \sin\theta + F_f \cos\theta \tag{1a}$$

$$W = F_n \cos\theta - F_f \sin\theta \tag{1b}$$

where F_n is the reaction force from curved surface to slider, the friction force component is F_f and θ is the rotation angle of slider. They are determined by the following Equation (2) and Equation (3)

$$F_f = \mu F_n \tag{2}$$

$$\sin\theta = \frac{u}{R} \tag{3}$$

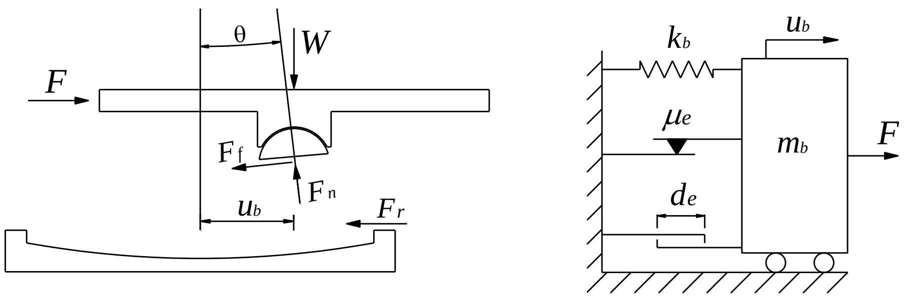

(a) (b)

Figure 3. The model of SFP bearing. (a) The forces and displacement, (b) Numerical model

It is assumed that the displacement *u* is sufficiently small compared to the radius *R* so that the rotation angle θ is very small, approximately: $\mu\sin\theta = 0$ và $\cos\theta = 1$ and combining Equations (1a) and (1b) can be written as:

$$F = \frac{W}{R}u + \mu W \tag{4}$$

In Equation (4), the (*Wu/R*) component is the restoring force. Accordingly, the horizontal stiffness k_b of the SFP bearing is computed as follows:

$$k_b = \frac{W}{R} \tag{5}$$

And the natural period of the SFP bearing is determined by:

$$T_b = 2\pi\sqrt{\frac{m}{k_b}} = 2\pi\sqrt{\frac{W}{gk_b}} = 2\pi\sqrt{\frac{R}{g}} \tag{6}$$

Apply impact force F_r to Equation (4), the equation governing the force - horizontal displacement relationship of bearing as shown following Equation (7)

$$F = \frac{W}{R}u + F_f + F_r \tag{7}$$

The hysteresis loop is shown in following Figure 4.

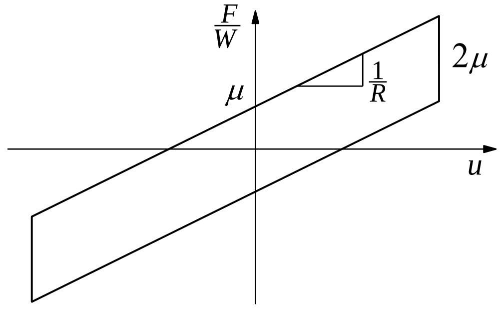

Figure 4. Hysteresis loop of SFP bearing.

With the inner force components of the bearing, the numerical model of bearing is an element with a combination of a spring element, friction element and gap element in parallel, as shown Figure 3(b). The linear spring stiffness k_b governed by Equation (5), friction element with friction coefficient μ_e and gap element governed by displacement limit $d_e = d$.

2.2. Modeling of seismic isolated structure with SFP bearing

The model of an *n*-story building is isolated by the SFP bearing. The slabs are assumed to be an absolutely rigid body. The structure is assumed to be symmetrical. Therefore, the rotational displacement effect is ignored. The 2-D model is applied to this structure. Each story have two degrees of freedom with the physical characteristics of: mass m_i, stiffness k_i, damping coefficient c_i and motion characteristics in two lateral directions of: displacement u_i, velocity $\dot{u}_i$ and acceleration $\ddot{u}_i$. The numerical model of base isolated structure has (2*n* + 2) degrees of freedom and is shown in Figure 5. The other assumptions considered for this model are as follows: The superstructure is linearly elastic, the behavior of the SFP bearing is nonlinear.

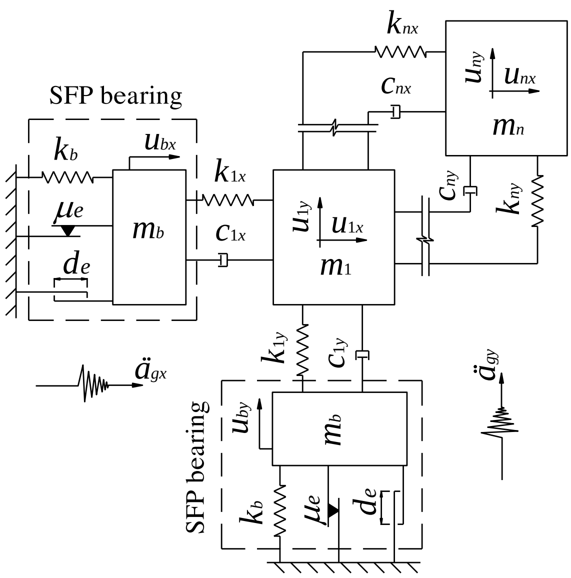

Figure 5. The 2-D model of seismic isolated structure with SFP bearing.

Mass m_b is the total mass of story above the bearing. It includes: base mass and equivalent to the mass of a floor.

Write the dynamic equations for each mass according to the D'Alembert principle, the equations of motion for the model in *x*-direction including (*n* + 1) equations can be expressed by:

$$\begin{cases} m_b(\ddot{u}_{bx}+\ddot{u}_{gx})+k_{bx}u_{bx}+F_{fx}+F_{rx}+k_{1x}(u_{bx}-u_{1x})+c_{1x}(\dot{u}_{bx}-\dot{u}_{1x})=0 \\ m_1(\ddot{u}_{1x}+\ddot{u}_{gx})+k_{1x}(u_{1x}-u_{bx})+c_{1x}(\dot{u}_{1x}-\dot{u}_{bx})+k_{2x}(u_{1x}-u_{2x})+c_{2x}(\dot{u}_{1x}-\dot{u}_{2x})=0 \\ \ldots \\ m_n(\ddot{u}_{nx}+\ddot{u}_{gx})+k_{nx}(u_{nx}-u_{n-1x})+c_{nx}(\dot{u}_{nx}-\dot{u}_{n-1x})=0 \end{cases} \quad (8)$$

The equations of motion for the model in *y*-direction is written similar to the *x*-direction.

The friction forces in the *x*-direction and *y*-direction are F_{fx} and F_{fy}, respectively. They can be written as follows [5].

$$\begin{cases} F_{fx}=\mu_e W Z_x \\ F_{fy}=\mu_e W Z_y \end{cases} \quad (9)$$

where the coefficient of sliding friction μ_e depends on sliding, which is modeled by the following equation [6]:

$$\mu_e=\mu_{\max}-(\mu_{\max}-\mu_{\min})e^{-\alpha|\dot{u}|} \quad (10)$$

where $\mu_{\max}$ and $\mu_{\min}$ are the sliding friction coefficients at maximum velocity and nearly zero sliding velocity, respectively, α (s/m) is a rate parameter for various conditions of Teflon-steel interface and pressure that controls the transition from $\mu_{\max}$ and $\mu_{\min}$ and $\dot{u}$ is the sliding velocity computed as [5]:

$$\dot{u}=\sqrt{\dot{u}_{bx}^2+\dot{u}_{by}^2} \quad (11)$$

Z_x and Z_y, which are bounded by the values ±1, are dimensionless hysteretic variables along the *x* and *y*-directions can be expressed as follows [5, 7]:

$$\begin{pmatrix} \dot{Z}_x Y \\ \dot{Z}_y Y \end{pmatrix}=\begin{pmatrix} A\dot{u}_{bx} \\ A\dot{u}_{by} \end{pmatrix}-\begin{bmatrix} Z_x^2(\gamma sign(\dot{u}_{bx}Z_x)+\beta) & Z_xZ_y(\gamma sign(\dot{u}_{by}Z_y)+\beta) \\ Z_xZ_y(\gamma sign(\dot{u}_{bx}Z_x)+\beta) & Z_y^2(\gamma sign(\dot{u}_{by}Z_y)+\beta) \end{bmatrix}\begin{pmatrix} \dot{u}_{bx} \\ \dot{u}_{by} \end{pmatrix} \quad (12)$$

where *Y* is the yield displacement, and *A*, β, γ and η are dimensionless constants and are determined from the experiment that control the shape of the hysteretic loop. These quantities can be specified as suggested by Constantinou et al [6], [8]: Y = 0.25 mm is the yield displacement, A = 1, β = 0.1, η =2 and γ = 0.9.

And the impact forces F_{rx} and F_{ry} can be written as follows [9]:

$$\begin{cases} F_{rx}=k_r(|u_b|-d_e)sign(u_x)H(|u_b|-d_e) \\ F_{ry}=k_r(|u_b|-d_e)sign(u_y)H(|u_b|-d_e) \end{cases} \quad (13)$$

where *H* is the value of the Heaviside step function, k_r is the impact stiffness after contacting the maximum horizontal displacement which should be assigned a large value and u_b is the radial displacement of bearing ($u_b=\sqrt{u_{bx}^2+u_{by}^2}$).

The motion differential equations are solved by the fourth-order Runge-Kutta numerical method, using the ***ode15s*** function in Matlab [10] to find the results of the time-history analysis.

3. Numerical example

To illustrate the behavior of a structure seismically isolated by SFP bearing subjected to earthquake and evaluate seismic effectiveness of SFP bearing for construction in Vietnam, an analysis of a mid-rise steel building subjected to ground motion acceleration records with ground conditions in Hanoi is implemented.

3.1. Parameters of the structure and SFP bearing

The structure of the analysis is a 5-storey steel building with the structural parameters as shown in Table 1. The damping ratio ξ = 2,5% is taken from the steel material. This structure is taken from the full-scale experimental model of Ryan et al. [11]. It is compatible with seismic base isolation technology and can represent many similar constructions. This is the symmetrical structure. Therefore, the stiffness is the same in the x- and y-directions ($k_x = k_y$).

Table 1. Parameters of the structure.

Story	1	2	3	4	5
Mass (kN.s^2/mm)	0.0824	0.0814	0.0811	0.0801	0.1199
Stiffness (kN/mm)	131	105	93.3	76.2	61.1

The parameters of the bearing are chosen on the basis of assumptions with reference from previous studies. It is in accordance with structural and ground conditions at site. These parameters are chosen as follows: R = 3000 mm; μ = 0.02 - 0.04; d = 500 mm.

3.2. Selecting and scaling ground motions

With the ground condition, according to the forecasts, earthquake in Hanoi is Level 8 followed by the Earthquake Magnitude Scale. According to Vietnam Standards TCVN 9386:2012, the design ground acceleration is taken a_g = 0.24g for ground types D (with the parameters: $v_{s,30}$ < 180 m/s and NSPT < 15 blows/30cm) [12], and the values of the periods T_b, T_c and T_d and of the soil factor S describing the shape of the elastic response spectrum are determined: S = 1.35; T_b = 0.2; T_c = 0.8 và T_d = 2 [12]. Figure 6 shows the elastic response spectra for ground types D.

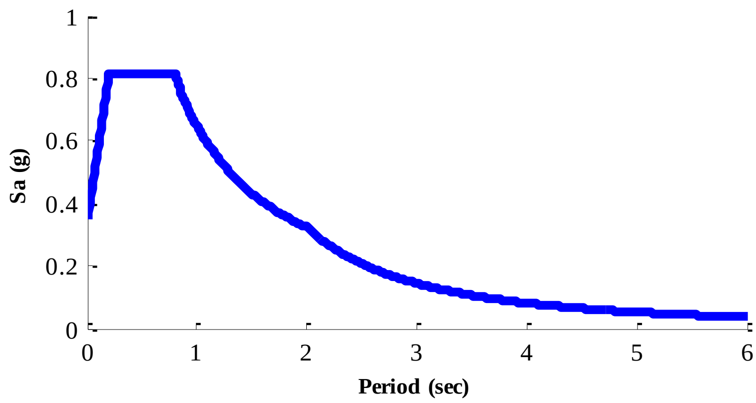

Figure 6. Elastic response spectra for ground types D.

The selection and scale of the magnitude of ground motion acceleration records in the time-history analysis is guided in ASCE 7-2010 (Section 17.3.2) [13] and is detailed by Naeim and Kelly [14]. Accordingly, the number of ground motion records is seven and the average value analysis will be selected as the design criteria. These values are combined by the square root of sum of squares (SRSS) method from x- and y-directions analysis results. In this study, the seven motion records selected from the The Pacific Earthquake Engineering Research Center (PEER) at the University of California, Berkeley [15], it is summarized in Table 2. These motions are recorded on ground types D.

The seven records will be multiplied by the SF factor to scale the average response spectrum matches the target spectrum according to Standards as shown in Figure 6. The SF factor is calculated as [16]:

$$SF = \frac{\int_{T_1}^{T_2} S_{aG} 1.3 S_{aC} dT}{\int_{T_1}^{T_2} S_{aG}^2 dT} \quad (14)$$

where S_{aG} and S_{aC} are response spectrum of motion and the target spectrum, respectively. T_1 to T_2 is effective periods range, is defined: with fixed-base structure $T_1 = 0.2T_f$, T_2=1.5T_f where T_f is the natural period of the structure in the fundamental mode, with base isolated structure T_1=0.5T_b; T_2=1.25T_b where T_b is the natural period of the base isolated structure.

Table 2. Ground motions for the analyses.

No.	Record Seq. #	Event (**ID**)	Year	Station	M_w	R_{rup}(km)	$V_{s,30}$ (m/s)	*PGA* (g)	
								X	*Y*
1	326	Coalinga-01 (**PAC**)	1983	Parkfield - Cholame 2WA	6.36	44.72	173.02	0.110	0.110
2	334	Coalinga-01 (**PAF**)	1983	Parkfield - Fault Zone 1	6.36	41.99	178.27	0.143	0.110
3	718	Superstition Hills-01 (**IVW**)	1987	Imperial Valley Wildlife Liquefaction	6.22	17.59	179	0.133	0.131
4	729	Superstition Hills-02 (**SUH**)	1987	Imperial Valley Wildlife Liquefaction	6.54	23.85	179	0.179	0.206
5	759	Loma Prieta (**FOC**)	1989	Foster City - APEEL 1	6.93	49.94	116.35	0.257	0.284
6	962	Northridge-01 (**WAT**)	1994	Carson - Water St	6.69	49.81	160.58	0.092	0.088
7	178	Imperial Valley-06 (**ELC**)	1979	El Centro Array #3	6.5	12.85	162.94	0.180	0.215

With the structure above, we calculate $T_{f\,=}$ 0.68 s, T_b is assumed to be about 2.7 s. This value will be checked after having the analysis results. If it is not satisfied, must be assumed again. The results of response spectrum of seven records for 2 cases: fixed-base and base isolated structure are shown in Figure 7. The target spectrum value S_{aC} is multiplied by 1.3 for considering the ground motion in both the *x* and *y* directions [12].

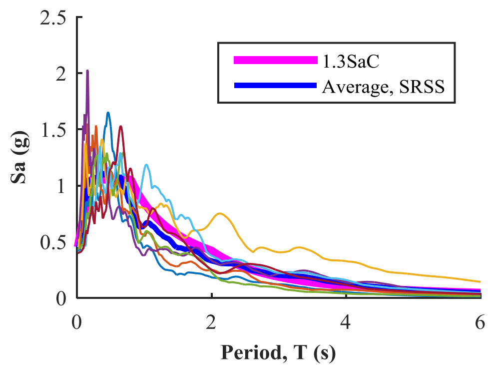

(a)

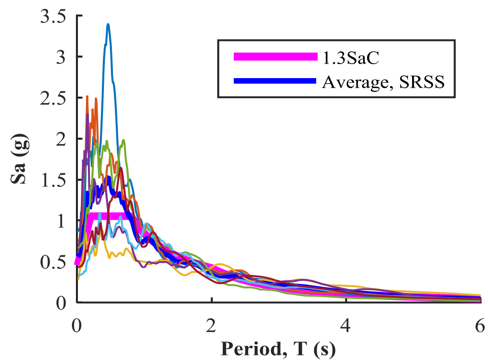

(b)

Figure 7. Target spectra compare to the median. (a) Fixed-base structure, (b) Base isolated structure.

3.3. Results and discussion

The Equations (8) present for the case of the base isolated structure. With the case of the fixed-base structure, the differential equations of motion are established similarly, it only consists of 2*n* equations (in this case, no mass m_b). The differential equations are resolved numerically using the Runge-Kutta method. However, for computational efficiency, the equations will be converted into the first order differential equations and solved by ODE functions (***ode15s*** solver) that are introduced in the research of Shampine et al. [10]. Accordingly, the results for the time history analysis of structure for two cases subjected to the seven ground accelerations are determined accurately. The average results are used to evaluate the behavior of the structure and the bearing.

Analytical values include: absolute acceleration of each floor, story shear force, total base shear and displacement of the bearing for two cases, and the effectiveness of the isolation system. These results are listed in Table 3.

Table 3. Isolation performance evaluation of SFP bearing.

Story		1		2		3		4		5	
		Val.	Red. (%)	Val.	Red. (%)	Val.	Red. (%)	Val.	Red. (%)	Val.	Red. (%)
Abs. acc. (g)	Fixed	0.67	64	1.14	82	1.64	88	2.14	91	2.58	90
	Isolated	0.24		0.20		0.19		0.18		0.25	
Inter. shear ($.10^3$ kN)	Fixed	7.27	94	6.84	94	5.98	93	4.70	92	3.03	90
	Isolated	0.42		0.41		0.40		0.36		0.29	
Base shear ($.10^3$ kN)	Fixed	7.27									
	Isolated	0.63 (Reduce: 91%)									
Base displ. (cm)	Fixed	0									
	Isolated	19.7									

The maximum absolute acceleration of each floor and the story shear forces of structure are shown in Figure 8. The data for this figure is the average value from 7 analysis.

The value of shear force in the 1st story in the time history analysis for two cases with ELC motion is shown in Figures 9 and 10. Similarly, the 5st story absolute acceleration is shown in Figure 11 and Figure 12.

The hysteresis loops represents the force - horizontal displacement relationship of the bearing is shown in Figure 13.

Figure 9 to 13 show the results of the analysis for ELC motion. With others, the results are similar, not shown here.

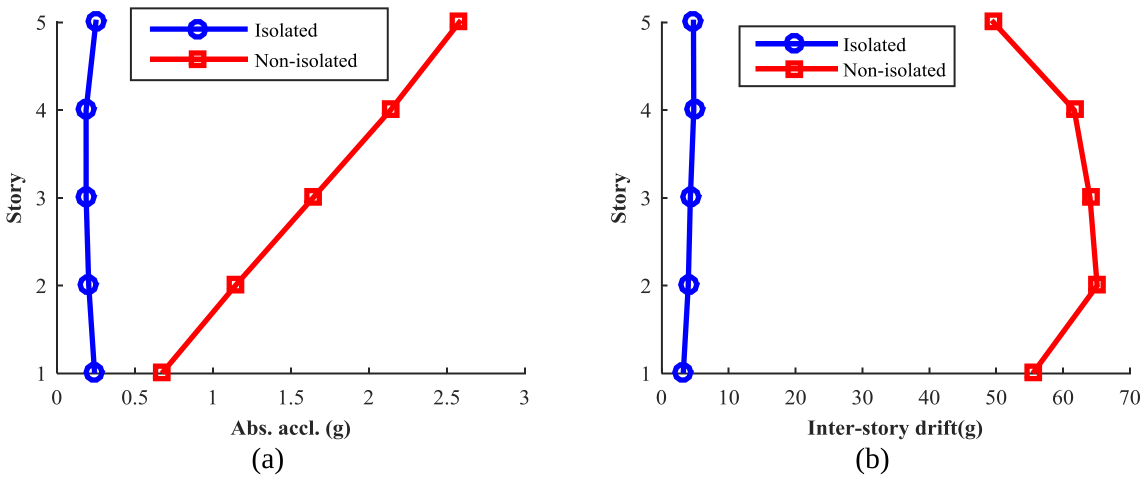

Figure 8. Effectiveness of SFP bearing. (a) Abs. acceleration of each story, (b) Inter-story drift

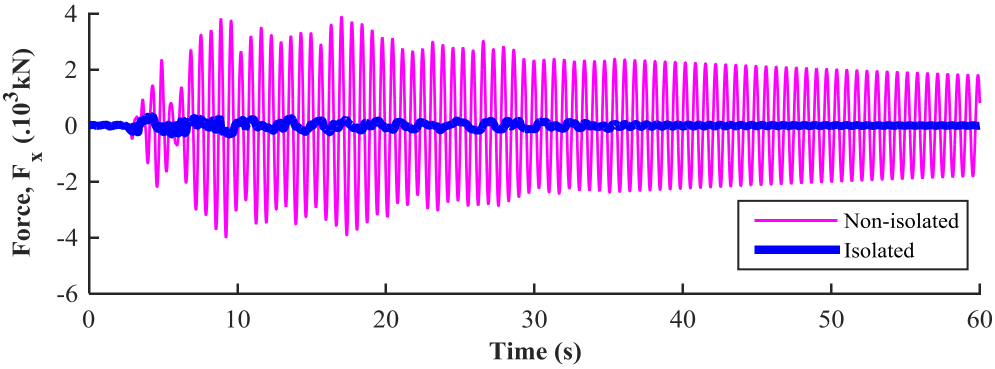

Figure 9. Shear force along *x*-direction F_x of 1st story with ELC motion

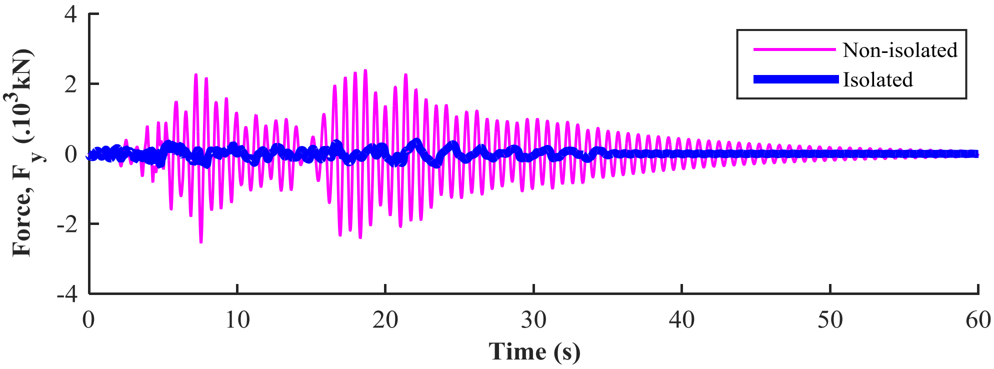

Figure 10. Shear force along *y*-direction F_y of 1st story with ELC motion

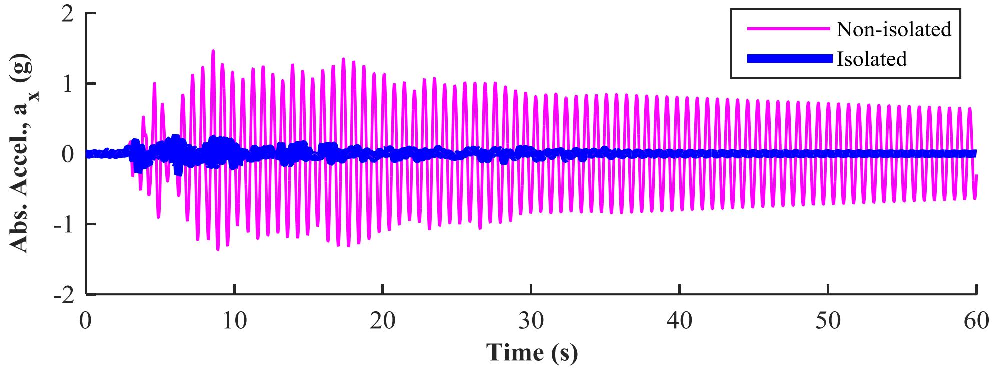

Figure 11. Absolute acceleration along *x*-direction a_x of 5st story with ELC motion

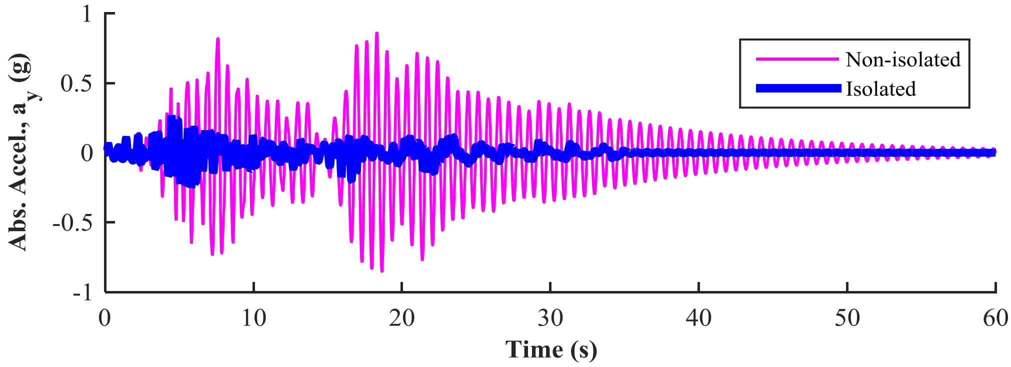

Figure 12. Absolute acceleration along *y*-direction a_y of 5st story with ELC motion

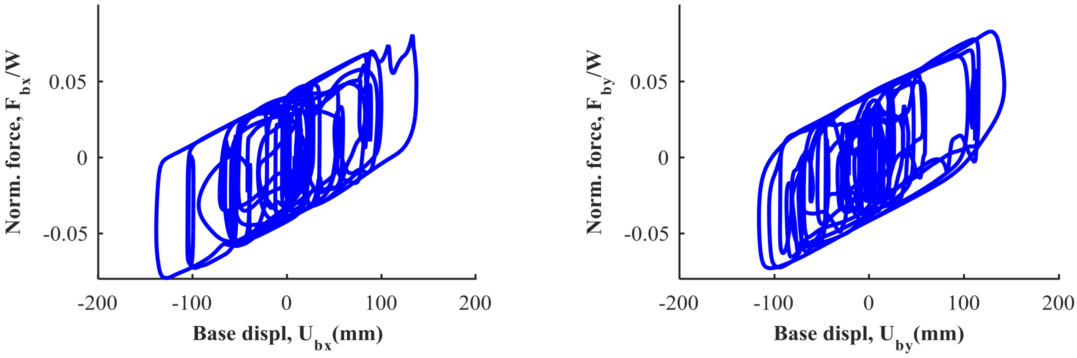

Figure 13. Hysteresis loops of bearing with ELC motion

According to the results shown in Table 3 and Figure 8, the seismic effectiveness of the SFP bearing is very high, approximately 85% for absolute acceleration in each floor and 90% for story shear forces. From the results, one can calculate the effective stiffness K_{eff} and effective period T_{eff} of the base isolated structure for each acceleration record according to the following formulas, respectively [17]:

$$K_{eff} = \frac{F_{\max}}{u_b} \tag{15}$$

$$T_{eff} = 2\pi\sqrt{\frac{W}{gK_{eff}}} \tag{16}$$

where F_{max} is the largest horizontal force in the bearing and u_b is the displacement at F_{max}.

The average value T_{eff} = 2.74 s will be compared with T_b = 2.7 s which is assumed initially. This result is slightly different, so the initial assumption value is reasonable, it doesn't need to repeat.

The displacement of bearing u_b = 19.7 cm is the basis for choosing the size of the bearing in the design. This displacement in base isolated buildings is usually large. This is a disadvantage of this technique. Therefore, the designer should note this problem.

With the time-history results in Figures 9 to 12, the seismic effectiveness is expressed throughout the time of the earthquake. At times with small ground acceleration, the movement of the bearing still occurs and seismic effectiveness is maintained. The shape of hysteresis loops in the analytical model shown in Figure 13 is similar with the results of research of Zayas [4], as shown in Figure 4.

4. Conclusions

The SFP bearing is very effective for earthquake-resistant design of buildings with the base isolation technology. This study propose a simple model to determine quickly the response of base isolated structures subjected to earthquakes using SFP bearing. Through this model, a time-history analysis is implemented for a 5-storey steel building subjected to ground motion acceleration records scaled to suit the ground conditions in Hanoi. The results point out that the effectiveness of the SFP bearing is very high, showing that the performance is over 85%. The dynamic responses of the structure show that absolute acceleration of each story, inter-story drift and base shear significantly reduce. Therefore, the use of this bearing in the seismic resistant design in Hanoi and in Vietnam general has promising perspective.

5. References

[1] Huong T 2014 *27 trận động đất ở Việt Nam trong nửa năm qua* http://vnexpress.net/tin-tuc/thoi-su/27-tran-dong-dat-oviet-nam-trong-nua-nam-qua-3035027.html
[2] Quang D 2011 *Hà Nội nằm trong vùng động đất cấp 7- 8* http://thanhnien.vn/thoi-su/ha-noi-nam-

trong-vung-dongdat-cap-78-432322.html.
[3] Wang P 2002 *Fundamentals of seismic base isolation* International training program for seismic design of building structures, sponsored by National Science Council, National Chiao-Tung Unversity, Hsinchu, Taiwan.
[4] Zayas, V, Low S and Mahin S 1987 *The fps earthquake resisting system: Experimental report* (*ucb/eerc* - 87/01) University of California, Berkeley.
[5] Nagarajaiah S, Reinhorn A M and Constantinou M C Nonlinear dynamic analysis of 3D-base-isolated structures *Journal of Structural Engineering* **117**(7) 2035 - 2054.
[6] Constantinou M, Mokha A and Reinhorn A 1990 Teflon bearings in base isolation II: Modeling, *ASCE Journal of Structural Engineering* **116**(2) 455 - 474.
[7] Park Y J, Wen Y K and Ang A 1986 Random vibration of hysteretic systems underbidirectional ground motions Earthquake *Engineering & Structural Dynamics* **14**(4) 543–557.
[8] Mokha A, Constantinou M C and Reinhorn A 1990 Teflon bearings in base isolation I: Testing, *ASCE Journal of Structural Engineering* **116**(2) 438 - 454.
[9] Fenz D and Constantinou M C 2008 Modeling triple friction pendulum bearings for response-history analysis *Earthquake Spectra* **24**(4) 1011-1028.
[10] Shampine F and Reichelt W 1997 The Matlab ode suite *SIAM Journal on Scientific Computing* **18**(1) 1 - 22.
[11] Ryan K and et al. 2013 *Full scale 5-story building with triple pendulum bearings at E-Defense* Network for Earthquake Engineering Simulation.
[12] Vietnam standards 2013 *TCVN 9386:2012 Design of structures for earthquake resistance* Publisher of Construction, Hanoi.
[13] American Society of Civil Engineers 2010 *Minimum Design Load for Buildings and Other Structures* ASCE 7-10.
[14] Naeim F and Kelly J 1999 *Design of seismic isolated structures: from theory to practice* John Wiley & Sons.
[15] Pacific Earthquake Engineering Research Center (PEER) 2017 *Ground motion database* http://ngawest2.berkeley.edu.
[16] Dao D 2012 *Seismic Response of a Full-scale 5-story Steel Frame Building Isolated by Triple Pendulum Bearings under Three-Dimensional Excitations* PhD Thesis University of Nevada.
[17] Fadi F and Constantinou M 2010 Evaluation of simplied methods of analysis forstructures with triple friction pendulum isolators *Earth. Engineering and Structural Dynamics* **39**(1) 5 - 22.

Acknowledgment
This research is funded by Industrial University of Ho Chi Minh City for research project under Grant No. 171.1051.